Journal of Sound and Vibration (1999) **220**(2), 365–377
Article No. jsvi.1998.1372, available online at http://www.idealibrary.com on IDEAL

LETTERS TO THE EDITOR

CHARACTERIZATION OF INTERFACIAL FORCES IN METAL-TO-METAL CONTACT UNDER HARMONIC EXCITATION

R. A. Ibrahim

Wayne State University, Department of Mechanical Engineering, Detroit, MI 48202, *U.S.A.*

AND

S. A. Zielke and K. Popp

Universität Hannover, Institut für Mechanik, 3017 *Hannover, Germany*

(*Received* 10 *January* 1997, *and in final form* 22 *October* 1997)

1. INTRODUCTION

Friction force is generated when two surfaces slide relative to each other. This force can be separated into two types. The first has the usual retarding effect upon motion maintained by an external force, while the second actually starts and maintains another motion of a vibrating nature which is superimposed on the first. For example, the work done by a damper with a Coulomb friction of a sliding mass describing a sinusoidal motion $X(t) = X_0 \cos \omega t$ is $U_c = -4F_cX_0$, where F_c is the Coulomb friction force. If the Coulomb friction force is replaced by a linear viscous force given by the expression $F_c\dot{X}/|\dot{X}|$, where $|\dot{X}|$ denotes the velocity amplitude, one can show that the corresponding work done is $U_d = -\pi F_cX_0$. It is seen that U_c is greater than U_d, and accordingly the damping effect of a damper with a Coulomb friction is larger than that of a linear viscous dashpot. In both cases damping acts as a retarding force. Tondl [1] examined the effect of dry friction on the unstable equilibrium position of a linear single-degree-of-freedom system with negative damping and found that dry friction can stabilize the equilibrium position if the coefficient of negative damping does not exceed half the value of the critical damping. Similar conclusions were drawn for two mass systems with negative damping where dry friction is necessary to stabilize the equilibrium position. A wide range of friction related problems have been recently reviewed by Ibrahim [2], Armstrong–Helouvry *et al*. [3], Popp [4] and Ferri [5]. The majority of these studies considered a friction coefficient that does not vary with time.

Kilburn [6] used the Fourier transform of the time series analysis and a statistical analysis based on the Kolmogorov–Smirnov goodness-of-fit test to analyze the time variation of friction force. Both methods indicated that friction behaves like a random process and can be treated as a constant signal with superimposed white noise. The instantaneous coefficient of friction is normally distributed, and its mean and standard deviation are functionally related. Aronov *et al*. [7, 8] conducted another series of tests using a pin-on-disk type model. The measured friction force and velocity of the pin along the friction force were found to change

0022–460X/99/070367 + 12 $30.00/0

randomly with time. Three different regions of operation were observed. The first is a stable steady state friction process with no fluctuations. This region occurs when the normal load is low and below a critical value. The second is a region of unstable intermittent self-excited vibration. The friction force suddenly increases, with high frequency modulated oscillations at 889 Hz (squeal), then decreases to a lower level with a low frequency 240 Hz (chatter). This region exists when the normal load increases beyond a certain critical value. The third regime is characterized by high frequency self-excited oscillations.

This paper presents an experimental investigation of the friction damping for a dynamical system subjected to sinusoidal excitation. The main objectives are to characterize the stochastic nature of friction and to identify the model parameters based on experimental results. With these results, a numerical simulation is carried out to describe the friction damping influence on the system behavior under the influence of friction damping. Particular emphasis is given to describing the stochastic nature of friction in terms of probabilistic theory. The dependency of the system response on the excitation frequency and amplitude, and on the friction characteristics is examined.

2. EXPERIMENTAL INVESTIGATION

2.1. *Experimental model and tasks*

The experimental model consists of a rectangular aluminum block of mass $m = 1{\cdot}028$ kg and is carried by four leaf springs whose other ends are clamped to a base block; see Figure 1. The base block is guided by Thomson bearings with very low friction and very low constraint tolerances in the direction orthogonal to the direction of excitation. The excitation is applied using a VTS-600 electromagnetic shaker. The head of the shaker is connected to the base block by a rigid steel bar. In order to generate a uniform sinusoidal signal, which may be corrupted by the model motion, a closed loop control is used. The accelerometer signal is fed into the control device of a Spectral Dynamics ST1715 sine/random vibration control system. This controller regulates the received signal and controls the shaker in a closed loop to obtain accurate sinusoidal excitation. With this setup reactive forces by the model movement are compensated for by the closed loop feedback control system.

The friction elements consist of two small hardened steel rods welded onto a leaf spring. The leaf spring is fixed to a non-rotating micrometer which carries a

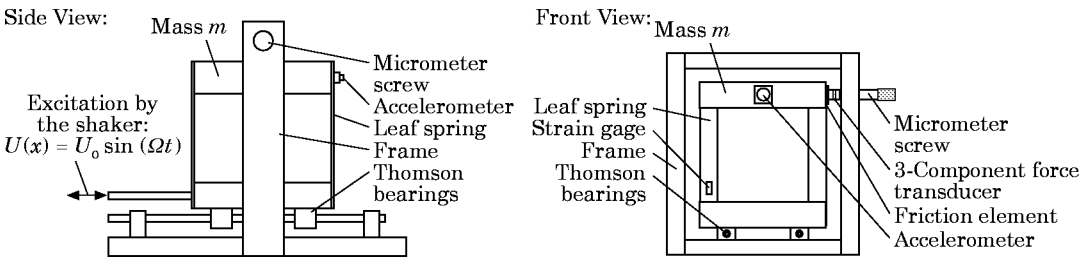

Figure 1. Schematic diagram of the model and its supporting rig.

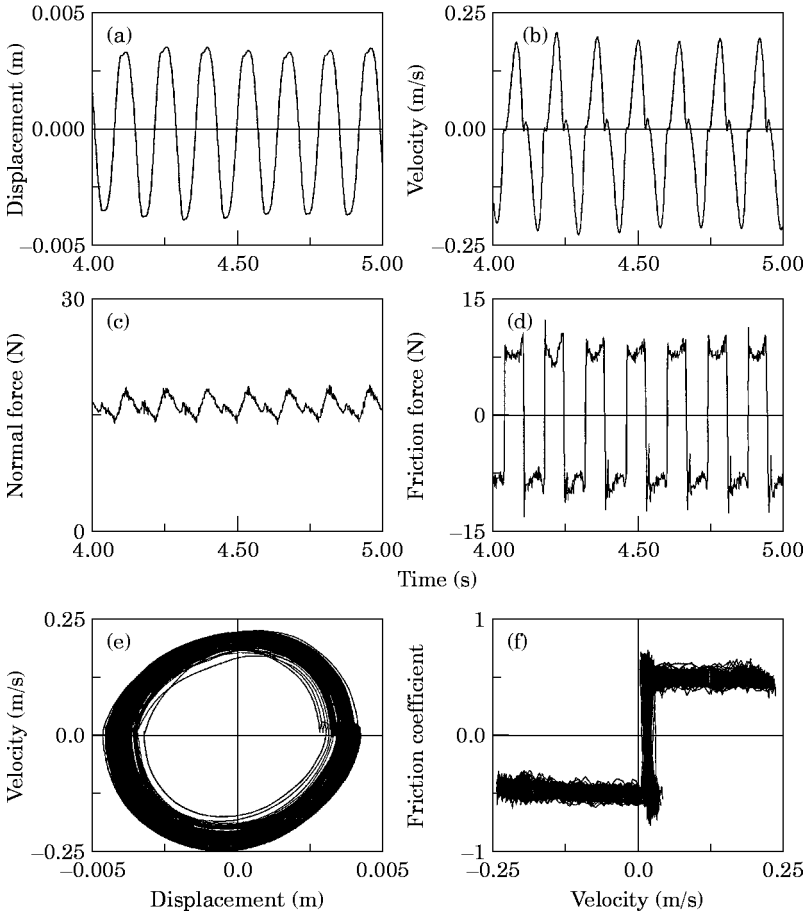

Figure 2. Experimental measurements of response and contact forces for relatively high normal force (excitation frequency 7 Hz, and excitation amplitude 2·5 mm). (a) Response displacement, (b) response velocity, (c) normal force, (d) friction force, (e) response phase portrait, and (f) friction–velocity curve.

three-dimensional Kistler type 9251A piezoelectric force transducer. A normal force can be applied by turning by a micrometer screw a friction plate which is screwed onto one side of the model block. An increase of displacement through the micrometer screw will result in a steady increase of the normal force through the deflection of the leaf spring. The friction plate material was changed from brass to steel to increase the hardness and therefore reduce the wear of the plate.

Transducer signals are received by a Data Translation model DT-2828 analog/digital converter board installed in an expansion slot of a 4DX2-66V Gateway 2000 personal computer. The signals come from (1) a Brüel & Kjaer model 4383 piezoelectric accelerometer mounted on the shaker platform, (2) a type CE-06-250UW-350 strain gage placed on one of the leaf spring beams in a half-bridge configuration to detect the model response, and (3) the normal and friction force components measured by a three-dimensional force transducer. The signals from the force transducer are amplified using a Kistler type 5814A10 three-channel charge amplifier. The signals are in the form of voltages, and are converged first into binary and then digital numbers. The digitized signals are

processed for estimating statistical parameters by using Interactive Laboratory System (ILS, by Signal Technology, Inc.) and Data Translation Visual Engineering Environment (DTVEE, by Data Translation Inc.). The board has four channels with a simultaneous sampling rate of 100 000 samples/s. To optimize the use of the PC for data processing, the ILS software package was also installed in a SUN Sparc-Station-10 which receives the acquired data via a network line for fast processing.

The relative displacement between the friction plate and the friction element can be calculated using the relationship

$$x_{rel} = -\ddot{x}(t)/\omega_0^2 + x_{str}, \tag{1}$$

where x_{str} is the displacement measured by the strain gage and x_{rel} is the calculated relative displacement with respect to the friction elements. The excitation acceleration $\ddot{x}$ is filtered to reduce the influence of noise. Taking the derivative of this signal gives the relative velocity. In the actual experimental testing it was found that the vertical and lateral acceleration components of the mass m are very small compared with the acceleration along the excitation direction.

2.2. *Experimental results*

The test procedure involves free and forced vibration tests. The purpose of free vibration tests is to measure the model parameters. The constants of the model and friction elements without contact constitute natural frequencies and damping

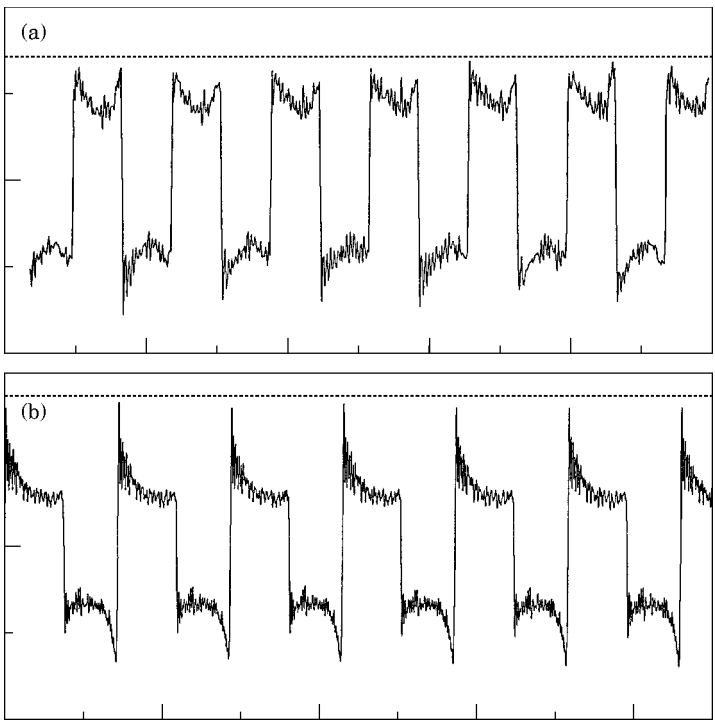

Figure 3. Time history records of the friction force plotted for two different sampling rates: (a) sampling rate 600 Hz, (b) sampling rate 100 000 Hz.

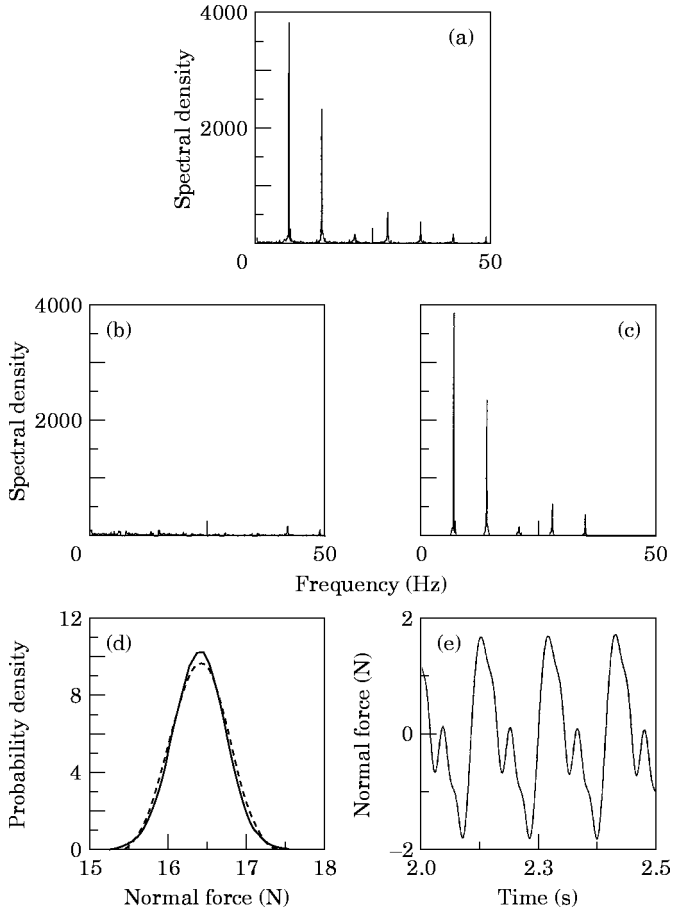

Figure 4. Characterization of the normal force under excitation frequency 7 Hz and amplitude 2·5 mm (corresponding to Figure 2(c)). (a) Power spectral density of the unfiltered signal, (b) spectral density after removing the first five periodic signals; (c) the first five periodic signals; (d) probability density of the normal force about its mean: minimum = 13·80 N, mean = 16·39 N, maximum = 18·10 N, variance = 0·1102; ——, Gaussian; ——, PDF; and (e) wave form of the normal force without the first five periodic signals.

ratios. These parameters are measured by performing free vibration tests. Based on these tests, the model natural frequency in the absence of friction element contact is found to be $f = 10{\cdot}05$ Hz, while the damping of the system is $\zeta = 0{\cdot}00225$.

The forced vibration measurements were taken for the shaker, model response, and friction and normal force components. The measured signals are processed to estimate statistics and amplitude–frequency response. Measurements have been taken for a fixed excitation amplitude and frequency but with varied applied normal force. Each set of data represents a time history with a sampling frequency of 600 Hz taken over a period of 50 s. Each measured signal was divided into 30 000 points which were found to be adequate to estimate the statistical parameters of response and contact forces.

2.2.1. *Characterization of the response*

Experimental measurements included normal and friction forces, model relative displacement as detected by the strain gauges, and relative displacement between the friction element and the model block as estimated by relation (1) and the corresponding relative velocity. Figure 2 shows time history records of the model relative displacement, relative velocity, and the corresponding phase diagram for two different normal load levels and under a constant excitation amplitude of 2·5 mm and a frequency of 7 Hz. The figure also includes the corresponding time history records of the normal and friction forces, and the dependence of the friction force on the relative velocity. Although the normal force was applied by initial constant pressure exerted by the forward displacement of the micrometer, its value experiences time variation during the same test. This variation is due primarily to the wear effects when significant amounts of material particles accumulate on the surface. This process is accompanied by the generation and elimination of surface asperities on the sliding surfaces. For this reason, the test had to be repeated after cleaning and polishing the surfaces. This variation is random in nature and fluctuates about a mean value. The corresponding friction is periodic with a superimposed random fluctuation. Accordingly, the dependence of the friction force on the relative velocity is not given by a single curve and the friction force possesses multivalues for the same relative speed. As the normal load level increases, the relative displacement experiences periodic nonlinear wave form. This is mainly observed in regions of high displacements, where complex dynamic

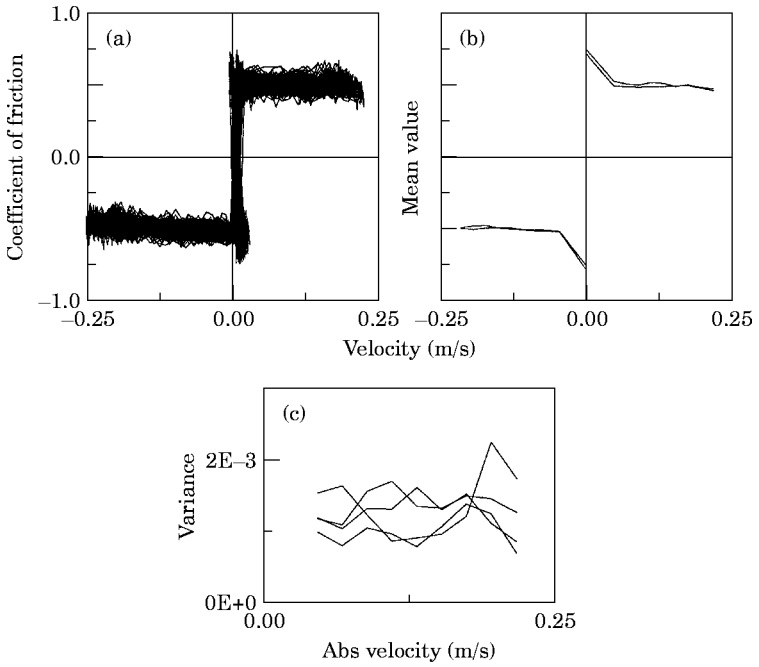

Figure 5. Dependence of friction coefficient on the relative velocity corresponding to Figure 2(d): (a) actual friction coefficient-velocity curves, (b) dependence of the mean value of the friction coefficient on the relative velocity, (c) dependence of friction coefficient variance on the relative velocity.

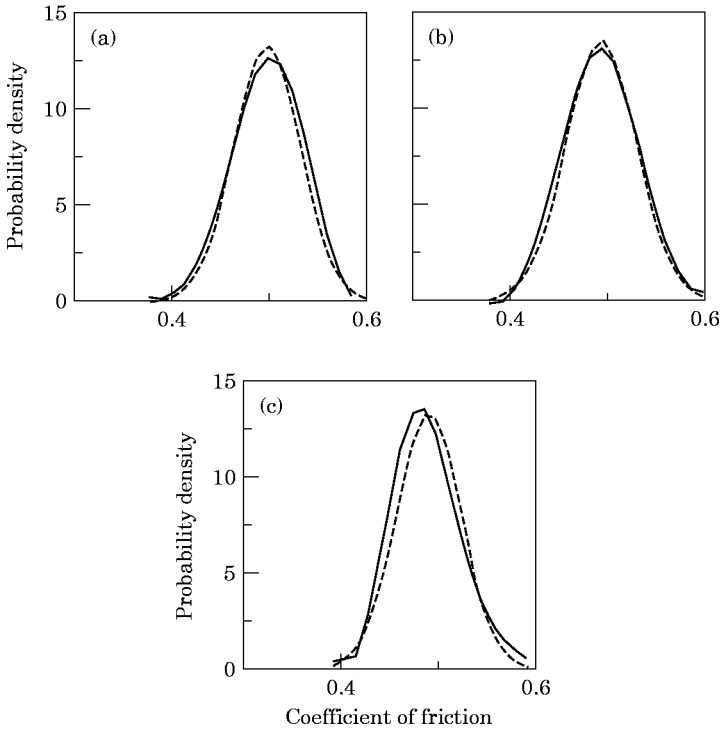

Figure 6. Probability density function of friction coefficient corresponding to Figure 2, for different values of the relative velocity (dotted curves show the corresponding Gaussian distribution): (a) 0·05 m/s, (b) 0·125 m/s, (c) 0·2 m/s.

characteristics take the form of stick–slip phenomena. This feature is clearly observed in both the time history records of the relative velocity and the corresponding phase diagram. In the neighborhood of zero relative velocity the state of stick–slip is clearly observed.

One may observe some kind of significant variation of the static friction forces in the time history records. A mgnification of the friction time history record is shown in Figure 3(a) for a sample frequency of 600 Hz. This apparent variation of the static friction force is fund mainly due to the sampling rate. Figure 3(b) shows the same friction time history record but with a sampling rate of 100 000 Hz. It is seen that the static friction force is almost the same. This is always valid in the present results.

2.2.2. *Characterization of the normal force*

Analyzing the normal force record, shown in Figure 2(c), reveals that the signal consists of periodic components superimposed on a random one, most likely of Gaussian distribution. Figure 4 shows the corresponding power spectra. The obvious peaks in the spectral density function represent the periodicity of the signal. With a self-programmed filter, the first five periodic signals are extracted from the time history, as seen in Figure 4(c), while the random component is shown in Figure 4(b). Figure 4(e) shows the remaining normal force components without the first five periodic components. The probability density function of the

normal force is shown by the solid curve in Figure 4(d). The dotted curve is the corresponding Gaussian distribution estimated from the mean and variance values. It is the normal displacements of the sliding surfaces which lead to a proportional change of the normal force through the deflection of the spring that carried the friction element.

Inspection of the frequency content of the normal force reveals that these frequencies are multiples of the excitation frequency. The first two frequencies which have the highest periodic influence on the normal force can be understood easily. The first frequency is mainly due to an unparalleled motion between the friction plate and the friction element. While an effort was made to achieve alignment between the friction element and the model surface, the inevitable small deviations resulted in some fluctuations, with frequencies identical to the excitation frequency. The second periodicity, with the frequency double the excitation frequency, is due to an uneven wear of the friction material. The rubbing surfaces will be subject to normal displacement as a result of the removal of surface

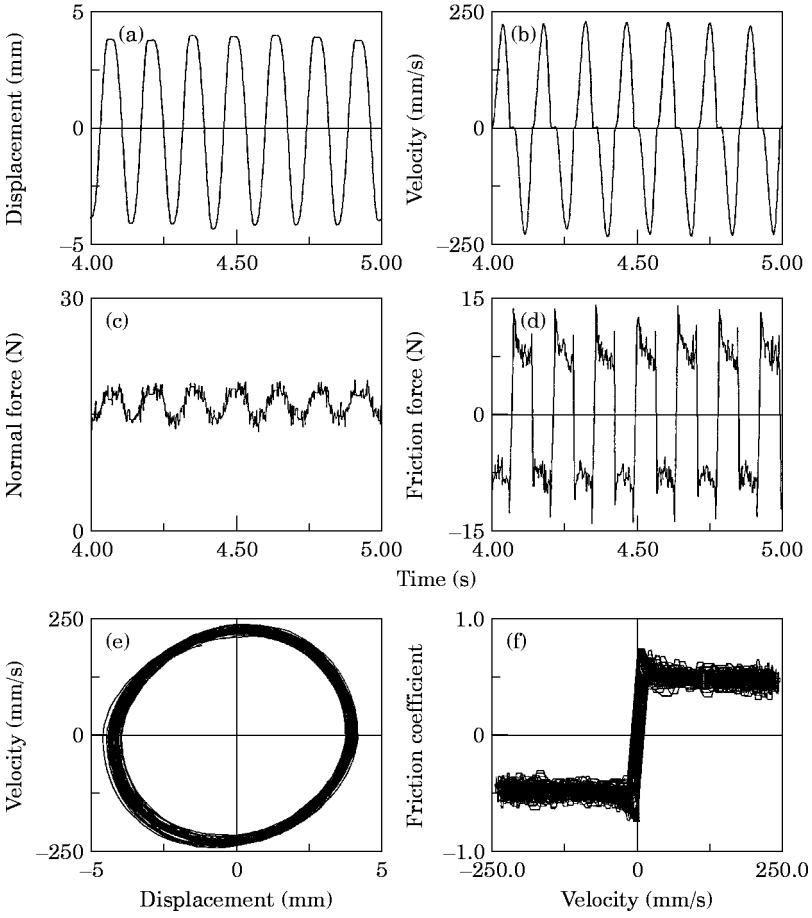

Figure 7. Numerical simulation results of response and contact forces (compare with Figure 2): (a) response displacement, (b) response velocity, (c) normal force, (d) friction force, (e) response phase portrait, and (f) friction-velocity curve.

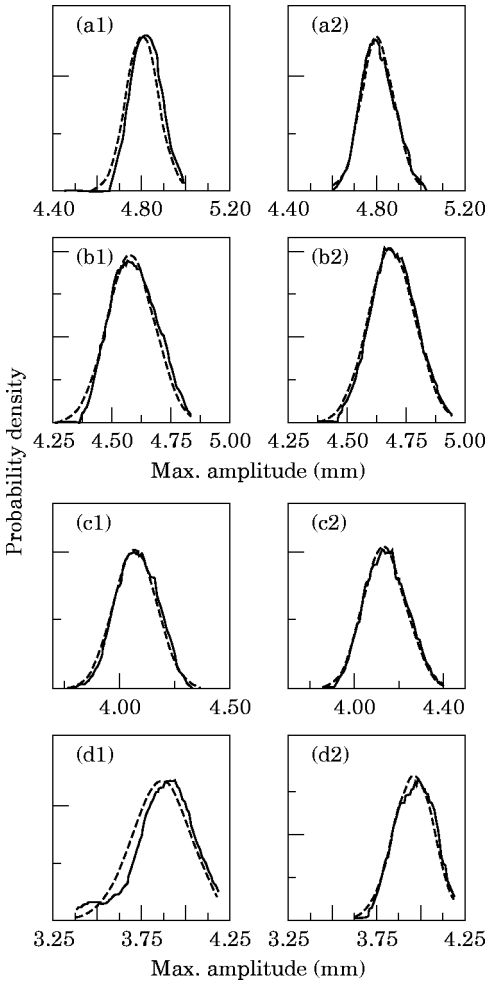

Figure 8. Comparison of measured and estimated probability density functions (pdf) of the response peak amplitude for different levels of normal force (Gaussian pdf is shown by dotted curves): (a1) measured normal load mean value $\mu_N = 7{\cdot}519$ N, variance $\sigma_N^2 = 0{\cdot}1815$ N^2, response amplitude mean value $\mu_{X0} = 4{\cdot}8055$ mm, response amplitude variance $\sigma_{X0}^2 = 5{\cdot}3825$E03 mm^2; (a2) simulation $\mu_N = 7{\cdot}519$ N, $\sigma_N^2 = 0{\cdot}1815$ N^2, $\mu_{X_0} = 4{\cdot}8056$ mm, $\sigma_{X_0}^2 = 5{\cdot}546825$E-3 mm^2; (b1) measured $\mu_N = 11{\cdot}5$ N, $\sigma_N^2 = 0{\cdot}1179$ N^2, $\mu_{X_0} = 4{\cdot}5855$ mm, $\sigma_{X_0}^2 = 1{\cdot}008$E-2 mm^2; (b2) simulation $\mu_N = 11{\cdot}5$ N, $\sigma_N^2 = 0{\cdot}1179$ N^2, $\mu_{X_0} = 4{\cdot}69103$ mm, $\sigma_{X_0}^2 = 1{\cdot}00155$E-2 mm^2; (c1) measured $\mu_N = 15{\cdot}3$ N, $\sigma_N^2 = 0{\cdot}0911$ N^2, $\mu_{X_0} = 4{\cdot}06913$ mm, $\sigma_{X_0}^2 = 9{\cdot}6615$E-3 mm^2; (c2) simulation $\mu_N = 15{\cdot}3$ N, $\sigma_N^2 = 0{\cdot}0911$ N^2, $\mu_{X_0} = 4{\cdot}132118$ mm, $\sigma_{X_0}^2 = 9{\cdot}35545$E-3 mm^2; (d1) measured $\mu_N = 16{\cdot}39$ N, $\sigma_N^2 = 0{\cdot}1102$ N^2, $\mu_{X_0} = 3{\cdot}854$ mm, $\sigma_{X_0}^2 = 2{\cdot}796425$E-2 mm^2; (d2) simulation $\mu_N = 16{\cdot}39$ N, $\sigma_N^2 = 0{\cdot}1102$ N^2, $\mu_{X_0} = 3{\cdot}9536$ mm, $\sigma_{X_0}^2 = 1{\cdot}5374$E-2 mm^2.

material. This will cause a frequency doubling of the displacement of the friction element which is periodically raised when it reaches its extreme ends. The other periodic influences are very likely caused by uneven surfaces such as bumps in the friction plate, or are the result of exciting the spring mass damper system of the friction element. Those periodic influences can be considered as external effects on the system and must be considered when comparing the results of the experiment with the simulation results.

2.2.3. *Characterization of friction*

The relationship between the normal force and the friction force gives the coefficient of friction. It is known that the coefficient of friction is highly dependent on a variety of parameters such as the relative velocity, normal force, surface conditions, temperatures, etc. In order to understand the stochastic nature of the coefficient of friction, the observed hystereses of friction–velocity, and its dependency on the normal force, the coefficient of friction is separated into four segments representing different states of positive and negative velocity and acceleration direction. These measurements are separated into segments within different velocity ranges. From the final data sets, the probability density function can be calculated and compared with a Gaussian distribution. Finally, the mean value and the variance are being plotted to show their dependency on the relative velocity. This procedure is being done for a variety of different normal forces to obtain the influence of the normal force on the coefficient of friction.

The dependency of the friction coefficient, its mean value, and its variance on the relative velocity are obtained for different levels of the normal force at discrete values of the relative velocity. Figure 5 shows a sample of these statistics for the case of Figure 2. Based on the ensemble of different measurements it was found that as the normal force increases the variance of the friction coefficient decreases. However, the probability density function of the friction coefficient deviates from Gaussianity as the normal load and relative velocity increase, as shown in Figure 6. Considering the limitations of data taken during every test, the results can be considered to represent a Gaussian distribution especially for relatively low normal force levels. With increasing normal force, it is found that the distribution deviates from normality. The mean value indicated on the probability density function curves shows the non-linearity and hystereses of the coefficient of friction with respect to the relative velocity.

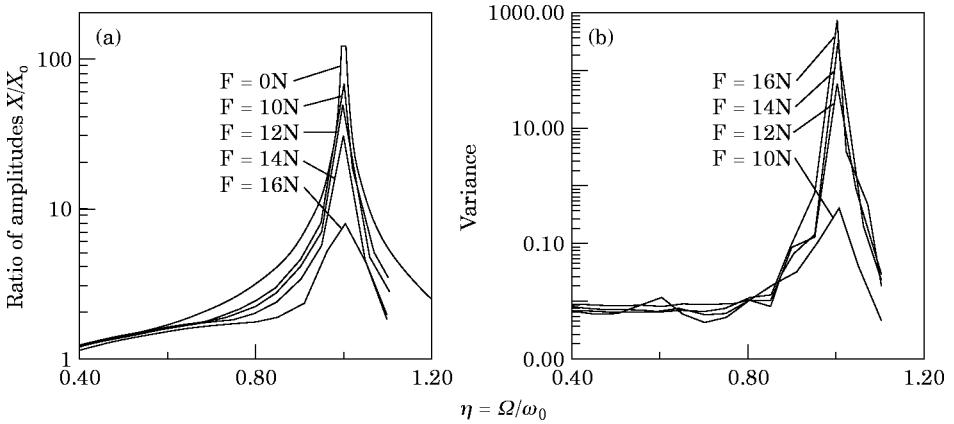

Figure 9. (a) Response amplitude-frequency curves for different levels of friction force, (b) dependence of response variance on excitation frequency for different levels of friction force.

3. ANALYTICAL MODELLING AND SIMULATION

The experimental model shown in Figure 1 can be analytically described by the equation of motion

$$m\ddot{x}(t) + c\dot{x}(t) + kx(t) = F_R + kU_0 \cos(\Omega t), \tag{2}$$

where m = block mass, x = displacement, c = damping coefficient, k = spring stiffness, F_R = friction force, U_0 = base excitation amplitude. The friction Force F_R depends on the velocity $\dot{x}$ and the normal force F_N. During the slip mode the friction force is

$$F_R = \mu F_N \operatorname{sgn}(\dot{x}), \tag{3}$$

whilst the following expression is used for the stick mode:

$$F_R = k(x(t) - U_0 \cos(\Omega t). \tag{4}$$

Introducing the non-dimensional parameters

$$\tau = \omega_0 t, \qquad \omega_0 = \sqrt{k/m}, \qquad \eta = \frac{\Omega}{\omega_0}, \qquad (*)' = \frac{\mathrm{d}(*)}{\mathrm{d}\tau} = \frac{(\dot{x})}{\omega_0}, \qquad \zeta = \frac{c}{2\sqrt{Km}},$$

equation (2) becomes

$$x''(\tau) + 2\zeta x'(\tau) + x(\tau) = (F_N/k)\mu + U_0 \cos(\eta\tau). \tag{5}$$

This equation can be written as three autonomous first-order differential equations

$$y' = \begin{bmatrix} y_1' \\ y_2' \\ y_3' \end{bmatrix} = \begin{bmatrix} y_2 \\ -2\zeta y_2 - y_1 + U_0 \cos(y_3) + (F_N/k)\mu \operatorname{sgn}(y_2) \\ \eta \end{bmatrix}, \tag{6}$$

where $y_1 = x(\tau)$, $y_2 = x'(\tau)$, $y_3 = \eta\tau$.

Equations (6) will be solved numerically. To achieve accurate results the simulation parameters have to be chosen to reflect the actual experimental results. It was shown that the normal force signal contains periodic and random components, whereas the coefficient of friction could be shown to be nearly Gaussian with a non-zero mean value. A subroutine using a random generator calculates a set of random numbers for a given mean value, and variance is developed. This subroutine is used to simulate the normal force and the coefficient of friction. The non-linearity and hystereses of the coefficient of friction can be represented by the expression

$$\mu(x) = a + b/(1 + c|\dot{X}|) + d\dot{x}^2 + R(\sigma_x^2), \tag{7}$$

where a, b, c and d are parameters used to fit experimental results and $R(\sigma_x^2)$ represents the Gaussian distribution with a variance σ_x^2.

The normal force is given as

$$F_N = F_{N,per} + R(\mu_x, \sigma_x^2), \tag{8}$$

where $F_{N,per}$ represents the periodic component while $R(\mu_x, \sigma_x^2)$ is the random component estimated for a given mean μ_x and variance σ_x^2.

The periodic normal force is only used to compare the simulation results with the experimental measurements. Because the periodic signals are specific to this model, they have not been used when obtaining general results for parameter dependencies and describing friction damping.

The friction appears as a force opposing the relative velocity in the equation of motion. It has random behavior which could be shown to be nearly Gaussian. For this reason the numerical simulation is performed to describe the system dynamic characteristics and to compare the response parameters with those measured experimentally. The friction damping simulation involves two states, the "stick" and the "slip" modes. The slip mode is solved numerically whereas the "stick" mode can be solved analytically. To determine the point of mode change between the "slip" and the stick" states, an iteration process is used. This procedure enables one to define a good approximation when the velocity reaches zero. The sign of the friction force is the signum of the velocity. This property can be easily inserted into the differential equation by a logical operator defined by the sign of the velocity. Furthermore, the randomness is taken into account by a random number generator. This generator is called up by a subroutine defined in the math library IMSL for FORTRAN, and generates a Gaussian distributed set of random numbers with a given mean value and variance. The random number then can be called at specified time intervals within the numerical integration.

The length of the time interval in which the coefficient of friction changes randomly can be varied and offers the possibility of adapting the simulation to meet the accuracy set by the experimental results. Using a random parameter in a simulation leads to random results. In general, when random problems like this are simulated, procedures like the Monte Carlo simulation are being used. Simulations like these require several numerical simulations to obtain a mean solution out of the varied set of random solutions. In the case of this simulation, the variable of interest is not the time history of displacement, but rather the distribution of maximum amplitude. For this case it is possible simply to run the simulation once for a long period of time and statistically analyze the distribution of the maximum amplitudes. These results can then be compared with experimental results.

Figure 7 shows the computational results calculated by using the information about the distribution of the normal force and the coefficient of friction. It is seen that the simulation results are in good agreement with the corresponding experimental results given in Figure 2. For better comparison, the maximum amplitude of the response is used as the main variable to describe the effect of friction damping. Figure 8 shows probability density plots of the maximum amplitude for the experiment and its corresponding simulation results. The distribution can be seen to have the main characteristics of a Gaussian distribution, but deviates as the normal force increases. Figures 9(a) and 9(b) show the dependence of the response amplitude and its variance on the excitation frequency for different friction force levels. The damping effect on the resonance response amplitude is noticed as the friction force increases.

4. SUMMARY AND CONCLUSION

The analysis of the experimental results has shown that the friction force can be described by a periodic component with superimposed random fluctuations. The random component has essentially a Gaussian distribution for relatively low levels of normal force. As the normal force increases, the distribution of the friction force deviates from normality. The mean value of the friction force is found to depend on the relative velocity in a non-linear form associated with hystereses, depending on the acceleration direction. Gaussian distributions of normal and friction forces are used for numerical simulation. This is not an exact assumption for increasing normal forces, which is reflected by the results obtained for higher normal forces in their deviation from experimental results. During experimental investigation it was hard to achieve repeatability of results. Conditions such as surface roughness and unevenness are the main sources of changing experimental conditions. Since their influences on the system response are very high, it is very difficult to reach exact conclusions about the system's behavior. Furthermore, the experimental setup was found to be very sensitive with respect to applying a constant normal force. Large periodic fluctuations of the normal force did not allow a proper evaluation of the influence of the magnitude of the normal force on the coefficient of friction.

ACKNOWLEDGMENTS

This research has been supported by a grant from the National Science Foundation under grant No. INT-9311774. Partial support has also been provided by the Institute for Manufacturing Research at Wayne State University.

REFERENCES

1. A. Tondl 1970 *Self-Excited Vibrations*. Monograph No. 9, National Research Institute for Machine Design, Bechovice.
2. R. A. Ibrahim 1994 *American Society of Mechanical Engineers Applied Mechanics Reviews* **47**, 209–253. Friction-induced vibration, chatter, squeal, and chaos, part I: mechanics of contact and friction and part II: dynamics and modeling.
3. B. Armstrong-Helouvry, P. Dupont and C. C. de Wit 1994 *American Society of Mechanical Engineers Applied Mechanics Reviews* **47**, 275–305. Friction in servo machines: analysis and control methods.
4. K. Kopp 1994 *Zeitschrift für angewandte Mathematick und Mechanik* (*ZAMM*) **74**, 147–165. Nichtlineare Schwingungen Mechanischer Strukturen mit Füge-Order Kontakts-tellen.
5. A. A. Ferri 1995 *Special* 50*th Anniversary Design Issue*, *Transaction of the American Society of Mechanical Engineers* **117**, 196–206. Friction damping and isolation systems.
6. R. F. Kilburn 1974 *Journal of Lubrication Technology* **96**, 291–299. Friction viewed as a random process.
7. V. Aronov, A. F. D'Souza, S. Kalpakjian and I. Shareef 1983 *American Society of Mechanical Engineers Journal of Lubrication Technology* **105**, 206–211. Experimental investigation of the effect of system rigidity on wear and friction-induced vibrations.
8. V. Aronov, A. F. D'Souza, S. Kalpakjian and I. Shareef 1984 *American Society of Mechanical Engineers Journal of Tribology* **106**, 59–62. Interactions among friction, wear, and system stiffness—Part 2, vibrations induced by dry friction.